High-temperature resistant, ordered gold nanoparticle arrays

2006 Nanotechnology 17 2122

(http://iopscience.iop.org/0957-4484/17/9/008)

INSTITUTE OF PHYSICS PUBLISHING NANOTECHNOLOGY
Nanotechnology **17** (2006) 2122–2126 doi:10.1088/0957-4484/17/9/008

High-temperature resistant, ordered gold nanoparticle arrays

Danilo Zschech[1,6], Dong Ha Kim[2,3], Alexey P Milenin[1], Sigrid Hopfe[1], Roland Scholz[1], Petra Göring[1], Reinald Hillebrand[1], Stephan Senz[1], Craig J Hawker[4], Thomas P Russell[5], Martin Steinhart[1] and Ulrich Gösele[1]

[1] Max Planck Institute of Microstructure Physics, Weinberg 2, D-06120 Halle, Germany
[2] Max Planck Institute for Polymer Research, Ackermannweg 10, D-55128 Mainz, Germany
[3] Division of Nano Sciences and Department of Chemistry, Ewha Womans University, Seoul 120-750, Korea
[4] Materials Research Laboratory, University of California, Santa Barbara, CA 93106, USA
[5] Polymer Science and Engineering Department, University of Massachusetts, Amherst, MA 01003, USA

E-mail: zschech@mpi-halle.de

Received 12 September 2005, in final form 23 November 2005
Published 28 March 2006
Online at stacks.iop.org/Nano/17/2122

Abstract
Ordered gold nanoparticle arrays with high lateral density of 6.87×10^{10} nanoparticles cm^{-2}, which are stable up to temperatures of 600 °C, were fabricated. To this end, nanoparticles formed by thermal vacuum evaporation of Au were immobilized within the pores of nanoporous silicon wafers prepared by block copolymer lithography coupled with dry plasma etching. Even after high-temperature treatment the degree of order imposed by the block copolymer template was retained. Optionally, a nanoporous silicon nitride mask can cover the nanoporous silicon.

1. Introduction

Gold (Au) nanoparticles [1–3] have been used for various applications in nanoscience and nanotechnology. It is highly desirable to arrange them into well-ordered arrays. This may be accomplished by self-assembling block copolymer (BCP) films coupled with plasma etching and the use of thin porous alumina masks [4, 5]. Non-epitaxial systems with large Au clusters that are incommensurate with the underlying substrate show an extremely high diffusivity [6, 7]. For example, Au clusters on graphite surfaces have a mobility comparable to that of single adatoms. Even large islands formed from numerous clusters are still mobile. This behaviour is more pronounced at elevated temperatures [8]. Tan *et al* demonstrated that arrays consisting of Au particles with sizes ranging from 55 nm up to a few hundreds of nanometres and interparticle distances >100 nm fabricated by nanosphere lithography retain their order upon annealing at high temperatures [9]. However, Au mobility destroys any order imposed by lithographic processes when the particle size is decreased and the lateral density increased. This limits the usability of dense Au nanoparticle arrays for applications in the fields of plasmonics, sensor technology, catalysis and synthesis of nanowires. It still remains a challenge to fabricate Au nanoparticle arrays characterized by high lateral density of the particles and stability at high temperatures. Consequently, the mobility or coalescence of Au nanoparticles on a surface must be prevented without influencing the performance.

Here we report on Au nanoparticle arrays with a lateral density of 6.87×10^{10} nanoparticles cm^{-2} that retain their initial degree of order over a wide temperature range up to 600 °C. We discuss a configuration where an ordered porous layer of silicon nitride (Si_3N_4) on a Si wafer, formed by BCP templating, has potential use as an inert mask for the growth of dense, ordered arrays of Si nanowires by the vapour–liquid–solid method [10–13]. BCPs self-assemble into ordered arrays of nanoscopic domains, the nature of which depends on the composition of the BCP, having a characteristic period and size [14–24]. By removing one component, films of BCPs can be used as templates to pattern the underlying substrate. We used BCP lithography [25–30] coupled with dry plasma etching [31, 32] to generate ordered nanoporous Si. A liquid

[6] Author to whom any correspondence should be addressed.

eutectic Si/Au phase forms at temperatures above 363 °C. However, the growth of Si nanowires requires temperatures higher than the eutectic temperature. The pores within the Si substrate act as defects that pin the Au nanoparticles and the eutectic Si/Au droplets, respectively. The methodology presented here can be modified to meet the requirements of other device architectures. For other applications, such as catalysis and sensing, the Au nanoparticles or probes based on them must be exposed to a flowing medium. In such cases it would be advantageous to have pores with ∼1:1 aspect ratio. The process described is shown to be applicable to this case also.

2. Experimental details

2.1. Preparation of nanoporous silicon nitride-coated silicon wafers decorated with Au dot arrays

We used BCPs of polystyrene and polymethyl methacrylate (PS-*b*-PMMA) with a PS volume fraction of 0.7, a weight-average molecular weight (M_w) of 73 kg mol^{-1}, and a number-average molecular weight (M_n) of 67 kg mol^{-1} (Polymer Source Inc.) to produce the lithographic masks. A typical procedure to generate ordered arrays of pores decorated with Au nanoparticles is shown in figure 1. (100)-oriented Si wafers were coated with a 35 or 60 nm thick layer of Si_3N_4 by low-pressure chemical vapour deposition. By grafting a hydroxyl-terminated random copolymer of styrene and methyl methacrylate, P(S-r-MMA), on the surface, according to a procedure reported by Mansky *et al* [33], interfacial interactions of PS and PMMA were balanced. 1 wt% solutions of PS-*b*-PMMA in toluene were spin-coated onto these treated substrates to produce 35–40 nm thick films (determined by ellipsometry). The BCP films were heated for 2 days at 165 °C in an Ar atmosphere to orient the cylindrical PMMA domains normal to the film surface (figure 1(a)). The PMMA cylinders were selectively removed by UV irradiation followed by rinsing in acetic acid to produce a cross-linked PS film with 6.87 × 10^{10} pores cm^{-2}, having an average period of 42 nm, and a hole diameter of 25 nm [34–36]. The PS was stained with ruthenium tetroxide (RuO_4) [37] to increase the etch contrast of the nanoporous film on the substrate (figure 1(b)). The staining procedure produces an insoluble PS mask containing Ru atoms, which exhibits improved chemical and thermal stability. The pattern of this mask was transferred into the underlying Si_3N_4 by dry plasma etching for 44 s with a mixture of 10 vol% CHF_3 and 90 vol% Ar in an inductively coupled plasma (ICP) reactor (Oxford PlasmaLab System 100) equipped with 2.1 MHz ICP380 and 13.56 MHz RF sources. The positions of the holes etched into the substrate were determined by the positions of the pores in the BCP template (figure 1(c)). A 20 nm thick Au layer was then deposited onto the patterned substrate by thermal vacuum evaporation of Au for 20 s (deposition rate 1 nm min^{-1}) using an Edwards 306 system (figure 1(d)). To obtain pore walls consisting of hydrogen-terminated Si, we removed the native silica layer that forms under ambient conditions by etching with hydrofluoric acid prior to the decoration with Au. The lift-off of residual, Au-coated polymer film on the sample surface was performed with sharp blades. The stained PS mask could easily be removed because of its brittle consistency (figure 1(e)).

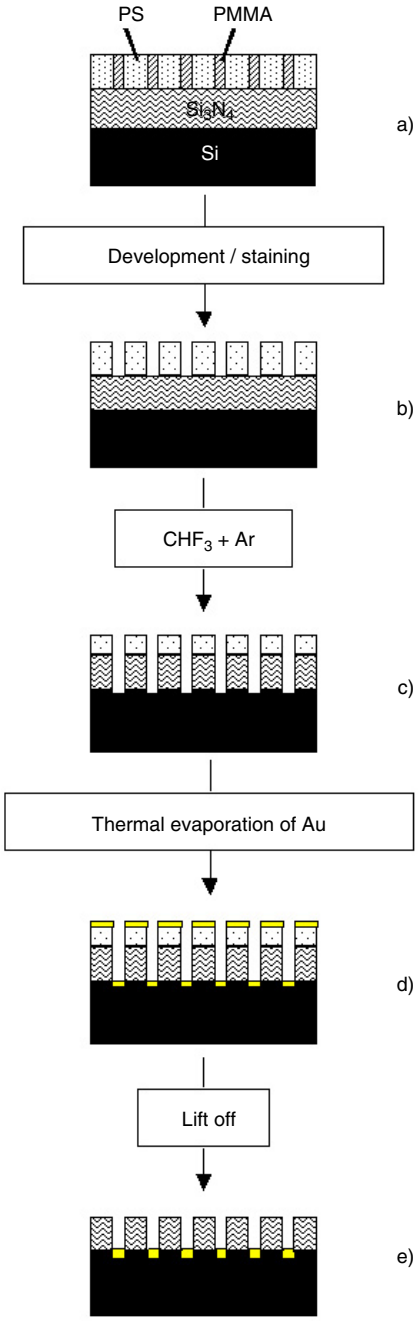

Figure 1. Schematic diagram of the fabrication procedure for high-temperature resistant Au nanoparticle arrays. (a) A film consisting of asymmetric PS-*b*-PMMA containing PMMA cylinders oriented normal to the film plane is formed on a Si wafer coated with Si_3N_4 and P(S-r-MMA). (b) An ordered porous PS film obtained by selective removal of the PMMA is stained with RuO_4. (c) The pore pattern is transferred into the wafer by dry plasma etching with a CHF_3/Ar mixture. (d) The sample is decorated with Au by thermal evaporation in high vacuum. (d) The polymer layer and the residual Au on the surface are lifted off.

(This figure is in colour only in the electronic version)

2.2. Preparation of bare nanoporous Si wafers decorated with Au dot arrays

A porous PS film was directly prepared on a bare (100)-oriented Si wafer. Further procedures followed those described

for the Si_3N_4-coated samples, except that the porous PS film was not stained and a mixture of 10 wt% c-C_4F_8 and 90 wt% Ar was used for the dry plasma etching (duration 40 s). The lift-off was performed by sonification in *N*-methylpyrrolidone for about 5 min.

2.3. Electron microscopy: scanning electron microscopy (SEM), transmission electron microscopy (TEM), and preparation of specimens

SEM was performed using a JEOL JSM 6300 F operated at an accelerating voltage of 5 kV. Cross-sectional specimens for TEM were prepared as follows: two pieces of the sample were glued face to face with epoxy resin and sliced with a diamond wire saw into approximately 400 μm thick sections. The sections were ground and polished to a thickness of approximately 80 μm, upturned, dimple-ground and further polished to a thickness less than 15 μm. The samples were then thinned to electron-transparency by ion milling from both sides with Ar (PIPS, Gatan). TEM was performed using a JEM 1010 operated at 100 kV.

2.4. Image analysis

Image analysis of the SEM images of the BCP films and Au dot arrays was performed using the program Digital Micrograph 2.5 (Gatan Inc.). A Fourier transform with an image size of 512 × 512 pixels was taken from the bottom part of the SEM image seen in figure 3(b). In the right-hand part of the diffraction pattern (see the inset) the modulus of the Fourier transform was azimuthally averaged. In a second step, a frequency profile was obtained by taking a line scan through the centre of the diffraction pattern thus treated. The branch representing the azimuthally averaged part of the diffraction pattern was used for the evaluation of the nearest neighbour relations.

3. Results and discussion

Figure 2(a) shows an SEM image of nanoporous Si. We used a wafer with a thin silica interlayer between the Si and the Si_3N_4. Etching the silica with aqueous hydrofluoric acid partially peels off the Si_3N_4 layer so that the underlying Si substrate is uncovered. On the left, the nanoporous PS template is shown, the uncovered Si_3N_4 layer is shown in the middle, and the patterned Si wafer underneath is seen on the right. Pores having diameters of ∼20 nm are shown easily penetrating through the Si_3N_4 layer. The indentations into the underlying Si are discernible at the bottom. Typical TEM images of cross-sectional specimens cut parallel to the long axes of the pores are shown in figure 2(b) (before Au deposition) and figure 2(c) (after Au deposition). The decoration with Au results in the formation of Au nanoparticles with diameters of ∼15 nm at the bottoms of the pores (figure 2(c)). The Au is in direct contact with the Si, since the native SiO_2 layer was removed prior to deposition by dipping the samples into an aqueous hydrofluoric acid solution.

To determine whether the Au nanoparticles are immobilized under conditions typically used for the growth of Si nanowires [38, 39], we annealed a sample under vacuum for

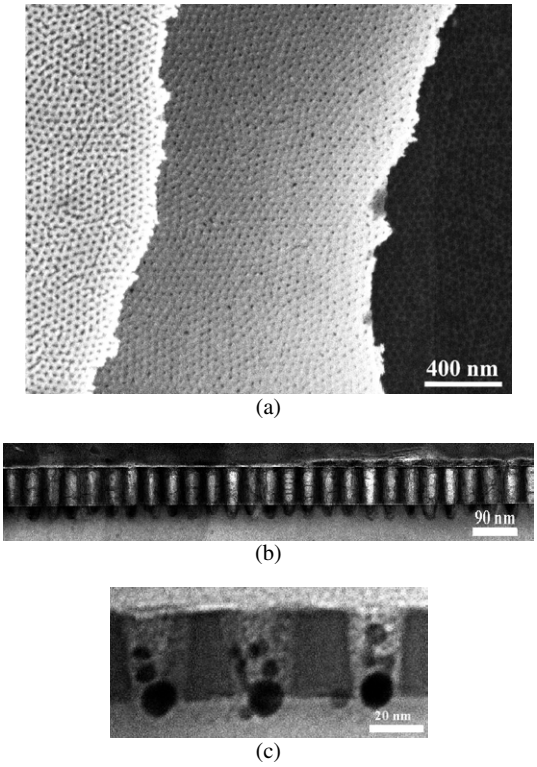

Figure 2. Electron microscopy images of nanoporous Si_3N_4-coated Si wafers after the dry plasma etching step, but prior to the thermal treatment. (a) SEM image showing the Au-coated porous PS film (on the left), the intermediate Si_3N_4 layer (in the middle), and the underlying Si wafer (on the right). ((b), (c)) TEM images of cross-sectional specimens of nanoporous arrays cut parallel to the long axes of the pores prior to and after the deposition of Au, respectively.

30 min at 450 °C. Since this temperature is above the eutectic point of Si/Au, a eutectic liquid forms during the heating, and Au recrystallizes upon cooling. An image, taken prior to the thermal treatment, is shown in figure 3(a). At the top, a nanoporous PS film uniformly covered with Au is seen, which covers the underlying Si_3N_4-layer. The bare Si wafer, which shows cylindrical wells containing Au nanoparticles, can be seen at the bottom. Etching away a thin SiO_2 interlayer separating the Si and the Si_3N_4 exposed this area. The Au nanoparticles appear brighter than the surrounding Si. During the annealing, the Au on the PS film formed large islands several tenths of a micron in size. However, on the patterned Si the ordered arrangement of the Au nanoparticles was conserved (figure 3(b)).

We determined the nearest neighbour distance in the array of annealed Au dots seen in the lower part of figure 3(b) by analysis of a Fourier transform taken from a quadratic image section (edge length approximately 1300 nm). The modulus profile (figure 3(c)) of the Fourier transform (figure 3(c), inset) shows a distinct peak corresponding to a distance of 41 nm in the real space, which can be attributed to the nearest neighbour distance in the Au nanodot array. The spacing of the Au nanoparticles thus corresponds to the period of the BCP template used.

The Au nanoparticles can also be immobilized within pores having small aspect ratios. A porous PS film was directly

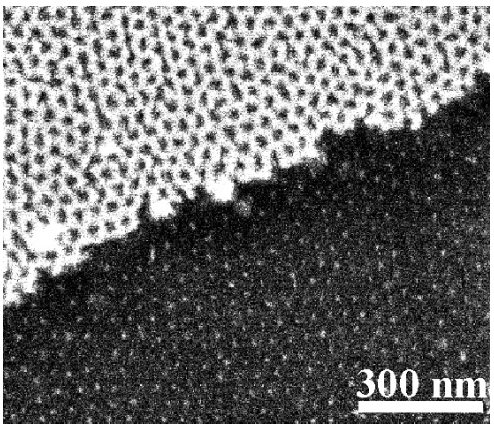

(a)

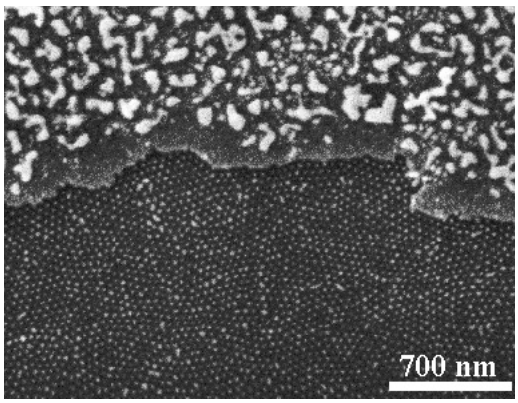

(b)

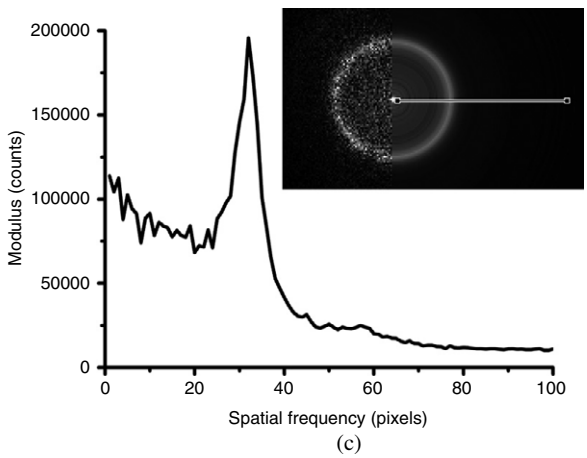

(c)

Figure 3. SEM images of wafers after dry plasma etching and decoration with Au. Au-coated porous PS films (at the top) and Au nanoparticles within the pores of ordered nanoporous Si (at the bottom) (a) prior to the thermal treatment and (b) after annealing at 450 °C for 30 min. (c) Modulus profile of the averaged Fourier transform (inset, right) obtained from a square section of the lower part of figure 3(b). The modulus profile was taken along the line indicated in the inset (zero-coefficient out of plotted range).

prepared on a bare (100)-oriented Si wafer, and the sample was further processed as described in section 2.2. The Si wafers thus obtained exhibited indentations with a diameter and a depth of approximately 20 nm, corresponding to an aspect ratio of one. After the deposition of Au, the samples were annealed

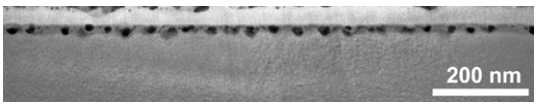

(a)

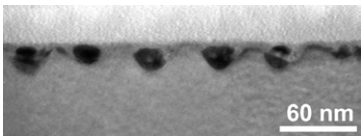

(b)

Figure 4. TEM images of cross-sectional specimens cut normal to the sample surface of nanoporous Si wafers, which were decorated with Au nanoparticles and then annealed at 600 °C for 30 min. (a) Overview; (b) detail.

under vacuum for 30 min at 600 °C. Cross-sectional TEM specimens, cut normal to the surface of the wafer, are shown in figure 4. The Au nanoparticles are seen to be located still within the indentations. Also, their initial diameter of 20 nm did not increase. Therefore, coalescence and diffusion of Au nanoparticles at high temperatures can be efficiently prevented by the approach presented here.

4. Conclusion

In conclusion, Au nanoparticles can be immobilized on Si at high temperatures within ordered dense arrays of nanopores prepared by using BCP templates. The procedure described also enables the fabrication of robust, temperature-resistant hybrid systems for applications in fields ranging from nanowire growth, sensor technology and plasmonics to catalysis. The long-range order as well as the lateral density of 6.87×10^{10} Au nanoparticles cm^{-2} can be altered and improved by manipulating the BCP used as a lithographic mask. Recent advances in assembling BCP films [40] make it possible to extend the approach presented here to a broad range of substrate materials. We assume that this method can also be applied to nanoparticles consisting of other metals, such as silver, platinum and palladium, since corresponding precursors could be reduced inside the nanopores.

Acknowledgments

The authors thank Ulrich Hilleringmann, Kornelia Sklarek, Klaus-Peter Meyer and Wilfried Erfurth for technical support as well as Kornelius Nielsch for fruitful discussions. This work was financially supported by Deutsche Forschungsgemeinschaft (DFG) in the frame of the Schwerpunktprogramm 1165 (SPP 1165: KN 224/15-1 & STE 1127/2-1).

References

[1] Brust M, Walker M, Bethell D, Schiffrin D J and Whyman R 1994 *J. Chem. Soc. Chem. Commun.* **7** 801
[2] Schmid G and Corain B 2003 *Eur. J. Inorg. Chem.* 3081
[3] Göring P, Pippel E, Hofmeister H, Wehrspohn R B, Steinhart M and Gösele U 2004 *Nano Lett.* **4** 1121
[4] Cheng G S and Moskovits M 2002 *Adv. Mater.* **14** 1567
[5] Sander M S and Tan L S 2003 *Adv. Funct. Mater.* **13** 393

[6] Bardotti L, Jensen P, Hoareau A, Treilleux M and Cabaud B 1995 *Phys. Rev. Lett.* **74** 4694
[7] Jensen P 1999 *Rev. Mod. Phys.* **71** 1695
[8] Lewis L J, Jensen P, Combe N and Barrat J L 2000 *Phys. Rev.* B **61** 16084
[9] Tan B J Y, Sow C H, Koh T S, Chin K C, Wee A T S and Ong C K 2005 *J. Phys. Chem.* B **109** 11100
[10] Cui Y, Lauhon L J, Gudikson M S, Wang J and Lieber C 2001 *Appl. Phys. Lett.* **78** 2214
[11] Gudiksen M and Lieber C M 2000 *J. Am. Chem. Soc.* **122** 8801
[12] Hochbaum A I, Fan R and Yang P D 2005 *Nano Lett.* **5** 457
[13] Gao D, He R G, Carraro C, Howe R T, Yang P D and Maboudian R 2005 *J. Am. Chem. Soc.* **127** 4574
[14] Spatz J P, Roescher A and Möller M 1996 *Adv. Mater.* **8** 337
[15] Glass R, Möller M and Spatz J P 2003 *Nanotechnology* **14** 1153
[16] Haupt M, Miller S, Glass R, Arnold M, Sauer R, Thonke K, Möller M and Spatz J P 2003 *Adv. Mater.* **15** 829
[17] Lazzari M and Lopez-Quintela M A 2003 *Adv. Mater.* **15** 1583
[18] Bates F S and Fredrickson G H 1990 *Annu. Rev. Phys. Chem.* **41** 525
[19] Hamley I W 2004 *Developments in Block Copolymer Science and Technology* (Chichester: Wiley)
[20] Morkved T L, Lu M, Urbas A M, Ehrichs E E, Jaeger H M, Mansky P and Russell T P 1996 *Science* **273** 931
[21] Muthukumar M, Ober C K and Thomas E L 1997 *Science* **277** 1225
[22] Thurn-Albrecht T, Schotter J, Kästle G A, Emley N, Shibauchi T, Krusin-Elbaum L, Guarini K, Black C T, Tuominen M T and Russell T P 2000 *Science* **290** 2126
[23] Krausch G and Magerle R 2002 *Adv. Mater.* **14** 1579
[24] Li X, Göring P, Pippel E, Steinhart M, Kim D H and Knoll W 2005 *Macromol. Rapid Commun.* **26** 1173
[25] Park M, Chaikin P M, Register R A and Adamson D H 2001 *Appl. Phys. Lett.* **79** 257
[26] Cheng J Y, Ross C A, Chan V Z H, Thomas E L, Lammertink R G H and Vancso G J 2001 *Adv. Mater.* **13** 1174
[27] Lammertink R G H, Hempenius M A, van den Enk J E, Chan V Z H, Thomas E L and Vancso G J 2000 *Adv. Mater.* **12** 98
[28] Guarini K W, Black C T, Milkove K R and Sandstrom R L 2001 *J. Vac. Sci. Technol.* B **19** 2784
[29] Kim D H, Kim S H, Lavery K and Russell T P 2004 *Nano Lett.* **4** 1841
[30] Shin K S, Leach K A, Goldbach J T, Kim D H, Jho J Y, Tuominen M, Hawker C J and Russell T P 2002 *Nano Lett.* **2** 933
[31] Blauw M A, Craciun G, Sloof W G, French P J and van der Drift E 2002 *J. Vac. Sci. Technol.* B **20** 3106
[32] Park M, Harrison C, Chaikin P M, Register R A and Adamson D H 1997 *Science* **276** 1401
[33] Mansky P, Liu Y, Huang E, Russell T P and Hawker C 1997 *Science* **275** 1458
[34] Thurn-Albrecht T, Steiner R, DeRouchey J, Stafford C M, Huang E, Bal M, Tuominen M, Hawker C J and Russell T P 2000 *Adv. Mater* **12** 787
[35] Guarini K W, Black C T and Yeung S H I 2002 *Adv. Mater.* **14** 1290
[36] Kim D H, Lin Z, Kim H C, Jeong U and Russell T P 2003 *Adv. Mater.* **15** 811
[37] Trent J S, Scheinbeim J I and Couchman P R 1983 *Macromolecules* **16** 589
[38] Schmidt V, Senz S and Gösele U 2005 *Appl. Phys.* A **80** 445
[39] Schmidt V, Senz S and Gösele U 2005 *Nano Lett.* **5** 931
[40] Ryu D Y, Shin K S, Drockenmuller E, Hawker C J and Russell T P 2005 *Science* **308** 236